

Classification of Retinal Cysts On SD-OCT Images Using Stacked Auto-Encoder

K. Alsaih^{1,2}, TB. Tang¹ and F. Mériadeau^{1,2}

¹Centre of Intelligent Signal and Imaging Research (CISIR)
Universiti Teknologi PETRONAS
32610 Bandar Seri Iskandar, Perak,Malaysia
Email: fabrice.meriaudeau@utp.edu.my

G. Lemaître², M. Rastgoo², D. Sidibé²

²LE2I, CNRS, Arts et Métiers
Univ. Bourgogne Franche-Comté,
71200, 12 rue de la Fonderie
Le Creusot, France

Abstract—Studies have shown that diabetes costs over \$ 770 million in USA. Diabetic retinopathy (DR) and its complication diabetic macular edema (DME) and age-related macular degeneration (AMD) are crucial diseases that might affect the retina and lead to blindness. Optical Coherence Tomography screening is one of the most effective screening methods to diagnose the retinal cysts lesions and to view the retina in 3-D volumes. This paper presents a methodology for automated detection of retinal cysts on Spectral Domain OCT (SD-OCT) volumes. The proposed method considers a generic classification pipeline that extracts the stable regions and then compares the stable regions with the optimal ground truth in order to label the potential regions. After that, the potential regions were resized and sent to the autoencoder to extract the features in an unsupervised fashion. Finally, the trained data was classified using the softmax layer in a supervised fashion, and the test data is passed through the network to validate the results. The results obtained from our pipeline are 93.0% and 82.0% for sensitivity (SE) and specificity (SP) respectively.

I. INTRODUCTION

Sugar level instability is what determine the existence of Diabetes in human body. Diabetes has two types: type 1 which is insulin-dependent and type 2 which insulin-independent. This critical disease is affecting many organs in the body like the Eye, Heart, Pancreas and others. Early detection and treatment of diabetic retinopathy (DR) and diabetic macular edema (DME) and age-related macular degeneration (AMD) play a major role to prevent adverse effects such as blindness. Screening programs on DR patients have been set up in many industrialized countries through the use of fundus images as well as optical coherence tomography (OCT) imaging. In United States, detection and curing the diabetese related to all types of eye diseases are estimated at almost 500 \$M [1] while frequent cases of DR expected to grow exponentially affecting over 300 M people worldwide by 2025.

Deep Networks like autoencoder and CNN could be the best in term of features learning, features extraction and dimensions reduction [2]. Most works done in OCT imaging related to the segmentation of the retinal layers and lesions and also in the classification of the SD-OCT B-scans using machine learning techniques like [3],[4]. To the best of our knowledge, detecting AMD method presented in this work has not yet addressed before. In this paper, we propose a solution for automated detection of AMD on Spectral Domain

OCT (SD-OCT) volumes using deep networks. Following this introduction, the rest of the paper is organized as follows: Sect. II focuses on the most recent works on the retinal cysts detection. Section III presents our classification framework while Sect. IV and Sect. V are respectively dedicated to data collection and the obtained results of our framework onto this dataset. The paper ends with a short discussion and conclusion in Sect. VI and VIII.

II. RELATED WORK

This section discusses the recent state-of-the-art methods for classification and segmentation of SD-OCT volumes as most of the recent contribution were done. An example of the data released to the OPTIMA (cyst segmentation) challenge is shown in Fig1.

The method proposed by Luis et al [5] is a machine learning based, where a model is trained using manual markings (to establish the ground truth) and then tested using another 15 volumes of testing data also provided by OPTIMA laboratory. In the preprocessing stage, the SD-OCT data was normalized and de-noised using non-local means filtering in the axial and horizontal direction. A fixed number of boundaries is defining the axial location of known intra-retinal layers are then automatically outlined using a developed segmentation algorithm done by Luis et al [6] (SOARS: Stanford OCT Automated Retinal Segmentation). A number of quantitative features (34 features) are extracted to characterize each volume located between the segmented internal limiting membrane (ILM) and inner segment junction (IS), where the possible cysts are located in. These features calculated at four different resolution levels to have set of predictors. After that, the risk score was calculated for each voxel. The final segmentation output is generated automatically by detecting an adaptive threshold to stratify the output scores in those belonging to a cyst or background. The accuracy using this method has achieved good results 80% of correctly segmented B-scan leading to a mean dice coefficients of 0.59.

Another proposed method by Ipek et al.[7], which is based on cost function (opposed to machine-learning) that generalizes well to a variety of images. This cost function takes into account the general characteristics of the input

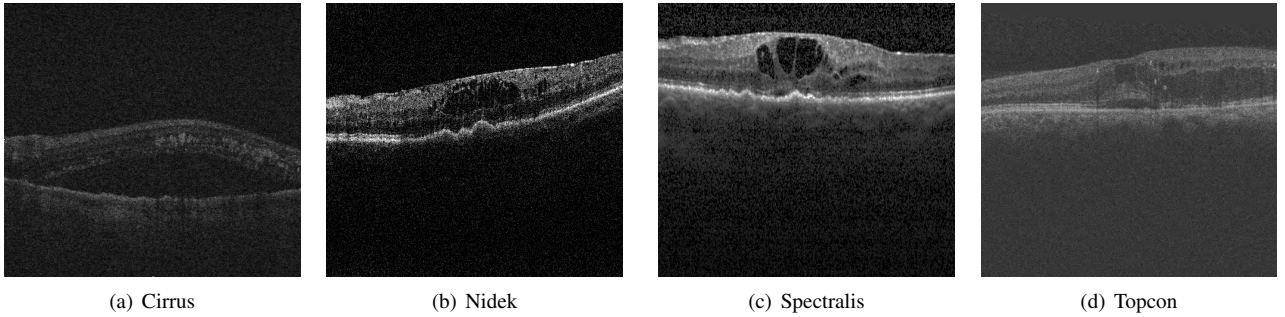


Fig. 1. Examples of SD-OCT images in OPTIMA challenge dataset.

image as well as the well-known characteristics of fluid-associated abnormalities. As the background and the cyst color in OCT images are black, most methods focused in specific regions on the B-scan slice which lie between the retinal layers specifically between the nerve fiber layer (NFL) and retinal pigment epithelium (RPE). The authors created a reliable mask even with the presence of fluid associated with cysts, followed by using a method to correct the Bruch membrane (BM). Then, a cost function is minimized to provide a segmentation of the B-scans and compared with the experts results. The method used fully covers all black holes that lie in the layers and it did not target cysts only.

Mahdad et al., [8] used a speckle noise reduction algorithm, which maintains strong edge sharpness and reduces the noise. This can be achieved by applying recursive Gaussian filter to noisy images and zero pixels value existing in the image are estimated from neighboring pixels lying in the retinal layers. After that, a threshold is used to the image to segment fluid space pixels. NFL and RPE layer are extracted in each B-scan. Finally, most of the possible false positives (FPs) are removed based on standard deviation of pixels intensity and morphology of the extracted candidate pixels. The results were validated using dice coefficients for the whole volume and they have achieved a mean dice coefficient 0.7099

Karthik et al. [9] started by de-noising the image by using Total Variational approach that reduced the texture content resulting in smooth piecewise constant images preserving the edges. Then, candidate selection using maximally stable extremal regions (MSER) is applied between NFL and RPE to save time and avoid unmeaningful and repeated regions in B-scan[10]. This feature computation produces a set of stable regions in an image. MSER is also used to detect the multi-scale objects without any smoothing. Both small and large structures can be detected based on threshold and other aspects based on the targeted regions to be extracted. A local descriptor is then assigned to each patch extracted by MSER which each region is bounded by a bounding box as the input for feature extraction. Finally , random forest classifier is used with fifty tree for results validation and the good results is produced when the number of cysts presented are in medium or large size and poor results for small cysts. This method achieved a mean dice coefficient of 0.3893.

A novel method using different way of training and extracting data was proposed by Venhuizen [11]. The method mainly uses Convolution Neural Networks to segment the images. Two stages define the process, in the first stage, three convolution neural networks (CNNs) are used to get a segmentation at different image scales. In the second stage, the three CNNs scale segmentations are fused together, redefining the borders of the segmented cysts by combining local information obtained with the lower scale network with contextual information obtained from the higher scale networks. Authors have validated their results using dice coefficients for the whole volume and they achieved an average of 0.728 and a sensitivity of 90%.

III. METHODOLOGY

In this part, we present the proposed method. A MATLAB code implementation is developed using the cluster provided by University of Burgundy with Xeon 2630 V3 processor, 128 GB of RAM and a GPU Nvidia Tesla K40 which processes the algorithms proposed in an average of 5 hours per experiment shown in Table 1. Inspired by the previous methods, our classification pipeline is depicted in Fig.2. The rest of the section presents into details each intermediate step.

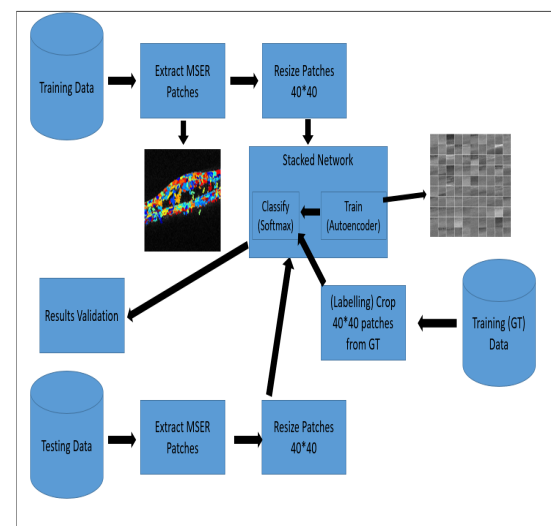


Fig. 2. Auto-encoder Network

A. Segmentation Process

This section explains the steps used to segment the B-scans as we intended to extract potential candidates in patch level. The full process applied to SD-OCT volumes as follows:

- 1) **Maximally stable extremal regions (MSER):** potential candidates regions are extracted for each B-scan, in the volume using MSER as shown in Fig.3.

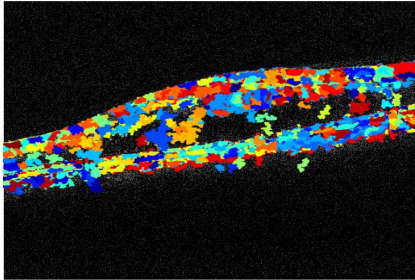


Fig. 3. Maximally stable extremal regions

- 2) **Simultaneous truth and performance level estimation (STAPLE):** the data provided includes two ground truths and STAPLE algorithm was used [12] to generate a single ground truth as shown in Fig.4.
- 3) **Labelling Patches:** Each patch extracted with the MSER is labelled to cyst or background according to the ground truth.

B. Auto-encoder Training And Feature Extraction

Auto-encoder is an unsupervised neural network which computes the hidden layer activations in the input level and measures the weight updates of the network using backpropagation. The patches fit to autoencoder were resized to 40x40 and the autoencoder has 100 and 50 neurons for the first and second hidden layers, respectively. The weights of this task can be shown in Fig.5.

After extracting the features from the two hidden layers, the training data was classified using the softmax layer in a supervised fashion using labels for the training data. Finally, the three separated trained components consisted of the encoders of the first and second hidden layers and the softmax layer are stacked to form the network. Classification of the testing patches were calculated by using the full network. After that, the results were validated using the confusion matrix into sensitivity and specificity.

IV. DATASET

The SD-OCT data used in this study is provided by the OPTIMA laboratory (Christian Doppler Laboratory for Ophthalmic Image Analysis, Department of Ophthalmology, Medical University of Vienna) for the Cyst segmentation challenge hosted at MICCAI 2015. These data consisted of 15 SD-OCT volumes containing a wide variety of retinal cysts with accompanying clinical ground truth annotation manually drawn by two different experts (Two Ground-Truths). The SD-OCT voxels have 4 different vendors for

TABLE I
Exp2 -AUTO-ENCODER RESULTS.

Threshold	Evaluation		
	Sensitivity	Specificity	Precision
Bigger than 150	0.93	0.53	0.68
Bigger than 150 + Fine tuning	0.93	0.82	0.85
Bigger than 190	0.94	0.51	0.67
Bigger than 190 + Fine tuning	0.95	0.75	0.80
Bigger than 200	0.94	0.54	0.69
Bigger than 200 + Fine tuning	0.95	0.79	0.83
Bigger than 400	1.00	0.00	0.55
Bigger than 400 + Fine tuning	0.72	0.26	0.54

training at different resolutions and scanning patterns: four volumes from Cirrus (Carl Zeiss Meditec, Dublin, CA, USA), three volumes from Nidek (NIDEK Co., Hiroishi, Gamagori, Japan), four volumes from Spectralis (Heidelberg Engineering, Heidelberg, Germany) and four volumes from Topcon (Topcon medical Systems, Santa Clara, CA, USA). Another 8 SD-OCT volumes were provided for testing: two volumes from each vendor specified above.

V. EXPERIMENTS AND RESULTS

This section explains the results in Table 1 outputted by auto-encoder and softmax layer classifier. This experiment starts by extracting the MSER regions from each image and roughly there are 50-200 regions extracted per B-scan. The MSER is extracted to cover almost all cysts appearing in the image and the number of extracted patches from the 15 SD-OCT volumes were 136,288 patches. After that, the extracted regions by MSER are cropped by finding the highest and lowest pixels value in the X,Y dimensions. The patches were resized to 40x40 in order to fit into autoencoder. Then, autoencoder is automatically trained to extract features in an unsupervised fashion.

Next, the MSER regions were extracted from testing data and then cropped similarly to the training data and the number of patches extracted from the testing data were 72,356 patches. These cropped regions were resized to 40x40 too. Then, test data were assigned to stacked-autoencoder network to evaluate the test patches. Fine tuning (back-propagation) is applied on the whole multi-layer network to minimize the error. Finally, the results were validated using confusion matrix and evaluated based on sensitivity, specificity and precision.

VI. DISCUSSION

The number of cysts presented in the data were varied in size, hence authors decided to try different thresholds for patch labelling based on the pixels appearing in the mask images. The results obtained are promising and the threshold of 200 pixels or more is giving good results. Lower threshold value of 150 overlapping pixels or higher than 250 will lead to unsatisfactory results. For 150, 200 and 250 overlapping

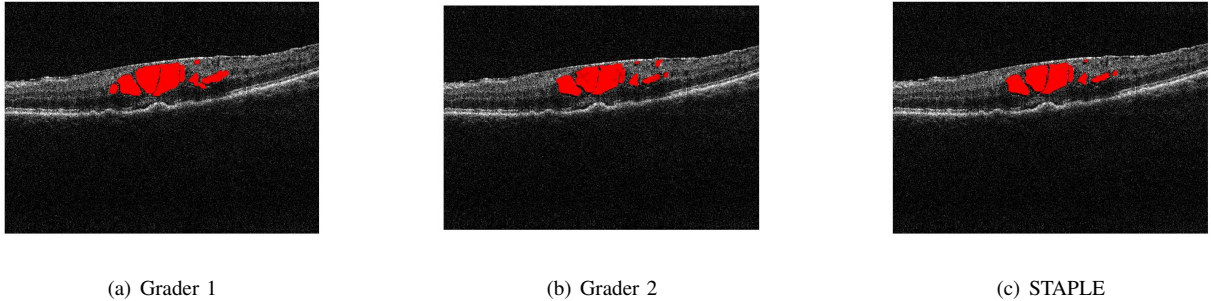


Fig. 4. Simultaneous truth and performance level estimation process

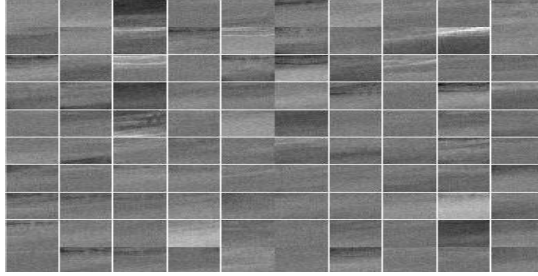


Fig. 5. Weights of Auto-encoder

pixels are giving a very good results as this number of pixels is representing the average of cysts size.

VII. CONCLUSION

We presented an automatic classification framework for SD-OCT volumes in order to identify retinal cysts. In this regard, the classification of potential regions of OCT images was based on extracting MSER and then compare it with the ground-truth given by the raters. Each volume has two ground-truths provided and STAPLE algorithm is applied to create one reference of ground truth based on the two ground-truths. After that, the patches were assigned to the auto-encoder for training and feature extraction before sending it to softmax layer for further classification of cyst appearance in image.

A recommended way to improve this study, is to denoise the image before extracting the MSER as the cysts are not fully covered. Also, make use of any adaptive techniques or implement the convolution neural networks instead of autoencoder.

VIII. ACKNOWLEDGEMENTS

This research was supported by Universiti Research Internal Fund (URIF) grant, Universiti Teknologi PETRONAS Malaysia.

REFERENCES

- [1] S. Sharma, A. Oliver-Hernandez, W. Liu, and J. Walt, "The impact of diabetic retinopathy on health-related quality of life," *Current Opinion in Ophthalmology*, vol. 16, pp. 155–159, 2005.
- [2] G. Litjens, T. Kooi, B. E. Bejnordi, A. A. A. Setio, F. Ciompi, M. Ghafoorian, J. A. van der Laak, B. van Ginneken, and C. I. Sánchez, "A survey on deep learning in medical image analysis," *arXiv preprint arXiv:1702.05747*, 2017.
- [3] K. Alsaih, G. Lemaitre, M. Rastgoo, J. Massich, D. Sidibé, and F. Meriaudeau, "Machine learning techniques for diabetic macular edema (dme) classification on sd-oct images," *Biomedical engineering online*, vol. 16, no. 1, p. 68, 2017.
- [4] M. Awais, H. Müller, T. B. Tang, and F. Meriaudeau, "Classification of sd-oct images using a deep learning approach," in *Signal and Image Processing Applications (ICSIPA), 2017 IEEE International Conference on*. IEEE, 2017, pp. 489–492.
- [5] L. de Sisternes, J. Hong, T. Leng, and D. L. Rubin, "A machine learning approach for device-independent automated segmentation of retinal cysts in spectral domain optical coherence tomography images."
- [6] L. de Sisternes, J. Hu, D. L. Rubin, and M. F. Marmor, "Localization of damage in progressive hydroxychloroquine retinopathy on and off the drug: Inner versus outer retina, parafovea versus peripheral fovearetinal layers in progressive hcq retinopathy," *Investigative ophthalmology & visual science*, vol. 56, no. 5, pp. 3415–3426, 2015.
- [7] I. Oguz, L. Zhang, M. D. Abràmoff, and M. Sonka, "Optimal retinal cyst segmentation from oct images," in *Optima Ophthalmic Image Analysis Challenge, Medical Image Computing and Computer Assisted Interventions (MICCAI) 2015*, 2016.
- [8] M. Esmaeili, A. M. Dehnavi, H. Rabbani, and F. Hajizadeh, "3d segmentation of retinal cysts from sd-oct images by the use of three dimensional curvelet based k-svd."
- [9] J. S. Karthik Gopinath, "Domain knowledge assisted cyst segmentation in oct retinal images," in *Optima Ophthalmic Image Analysis Challenge, Medical Image Computing and Computer Assisted Interventions (MICCAI) 2015*, 2015.
- [10] J. Matas, O. Chum, M. Urban, and T. Pajdla, "Robust wide-baseline stereo from maximally stable extremal regions," *Image and vision computing*, vol. 22, no. 10, pp. 761–767, 2004.
- [11] F. G. Venhuizen, M. Grinsvena, C. B. Hoyng, T. Theelen, B. Ginneken, and C. I. Sanchez, "Vendor independent cyst segmentation in retinal sd-oct volumes using a combination of multiple scale convolutional neural networks," *Medical Image Computing and Computer Assisted Intervention-Challenge on Retinal Cyst Segmentation*, 2015.
- [12] S. K. Warfield, K. H. Zou, and W. M. Wells, "Simultaneous truth and performance level estimation (staple): an algorithm for the validation of image segmentation," *Medical Imaging, IEEE Transactions on*, vol. 23, no. 7, pp. 903–921, 2004.